ENERGY AND POWER OF NONLINEAR WAVES IN A SEVEN STORY REINFORCED CONCRETE BUILDING

by

V. Gicev[a] and *M.D. Trifunac*[b]

a) *Rudarsko-geoloski fakultet, Goce Delcev 89, 2000 Stip, Republic of Macedonia*

b) *Dept. of Civil Eng., Univ. of Southern California, Los Angeles, California, 90089*

"The problem of designing structures to withstand destructive earthquakes is not in a very satisfactory condition. On the one hand engineers do not know what characteristics of the ground motion are responsible for destruction, and on the other hand seismologists have no measurements of seismic motion which are sufficiently adequate to serve for design, even if the destructive characteristics were known. Consequently, engineers have been forced to proceed on an empirical basis. From past experience… it has been found that buildings, which are designed to withstand a constant horizontal acceleration of 0.1 gravity are, on the whole, fairly resistant to seismic damage. It is fortunate that such a simple formula works at all…" Benioff [1934]

ABSTRACT

We note the limitations of the classical Response Spectrum Method (RSM) for design of earthquake resistant structures in the near field of strong earthquakes. The main one is that the RSM is based on the largest peak of the relative response, and does not consider the duration of strong motion. To illustrate an alternative approach the recorded response of a seven-story reinforced concrete hotel (VN7SH) in Van Nuys, California, damaged during January 1994, Northridge earthquake, is described in terms of one-dimensional layered shear beam model, undergoing nonlinear wave excitation. We use this model to show the time and space variations of wave energy and of power in the building response, and to set a physical basis for a new design method based on the power of strong motion pulses propagating through a building.

Keywords: Earthquake Response Spectra, Power of incident waves, Power Design method.

1. INTRODUCTION

Modern Earthquake Engineering began with the formulation of the concept of Response Spectrum by Biot, who presented the general theory (Biot 1932; 1933; 1934), analyzed the recorded accelerograms, and formulated the principles of response spectrum superposition (Biot, 1941;1942). Today, three quarters of a century later, his ideas still govern the principles of earthquake resistant design (Trifunac, 2003; 2005). Biot's method works well for the design of structures expected to vibrate without damage. However, pragmatic considerations, and optimization of cost result in the design of structures, which may experience damage from rare and very strong earthquake shaking. Thus, during the past 40 years, many modifications and "corrections" have been introduced into the Biot's response spectrum method to reconcile its *linear* nature with its desired *nonlinear* use in design (Veletsos and Newmark 1960).

At present much of the earthquake resistant design continues to be based on the linear concepts of relative response spectrum, and on mode superposition. However, as used in practice, the modal approach has a low-pass filtering effect on the end result (the computed peak relative displacement at each floor) because in design the higher modes are usually neglected. Therefore, in typical earthquake engineering applications the modal approach is not able to represent the sudden transient response. This is particularly so for excitation by high frequency pulses in the near-field, with large peak velocities, which are associated with high stress drop at the near asperities, and with duration short relative to the travel time required for an incident wave to reach the top of the building. Although, in principle, the representation of the linear response as a combination of the modal responses is mathematically complete, short "impulsive" representation would require considering infinitely many modes, which is impractical. The wave propagation methods are therefore more *natural* for representing the *early* transient response, and should be used to find solutions where the modal approach is limited.

Well-designed structures are expected to have uniformly distributed *ductile behavior* during the largest credible shaking, and *large energy reserve* to at least delay failure if it cannot be avoided. As the structure enters large nonlinear response, it absorbs the excess of the input energy by ductile deformation of its components. Thus, it is logical to formulate earthquake resistant design procedures in terms of the energy driving this process. In 1934, Benioff proposed the seismic destructiveness to be measured in terms of the response energy, which also can be related to the energy of strong motion (Arias, 1970; Trifunac and Brady, 1975a). Thus an alternative to the spectral method in earthquake resistant design is to analyze the flow of energy during strong motion. The principal stages of this flow include the earthquake source, the propagation path, and finally the remaining energy which leads to the response of a structure (Trifunac et al., 2001d).

The seismic energy associated with elastic waves radiated from the source (Gutenberg and Richter, 1956a,b) can be used to compare "sizes" of different earthquakes. This energy, E_s, is attenuated along epicentral distance, r, through the mechanisms of inelastic attenuation (Trifunac, 1994), scattering, and geometric spreading. The wave energy arriving towards the site is next attenuated by nonlinear response of shallow sediments and soil in the "free-field" (Joyner, 1975; Joyner and Chen, 1975; Trifunac and Todorovska, 1996; 1998a; 1999), before it begins to excite the foundation. The incident

wave energy is further reduced by nonlinear response of soil during soil-structure interaction (Gicev, 2005; Trifunac et al., 1999a,b; 2001a,b), and by radiation damping (Luco et al., 1985; Todorovska and Trifunac, 1991; 1992; Hayir et al., 2001).

Engineering analyses of seismic energy flow and distribution among different aspects of the structural response have been carried out since the mid 1950's. A review of the subject and examples describing the *limit-state* design can be found in the book by Akiyama (1985), and in collected papers edited by Fajfar and Krawinkler (1992), for example. In most engineering studies, the analysis begins by integrating the differential equation of dynamic equilibrium of an equivalent single degree of freedom system with respect to displacement, which results in

$$E_I = E_K + E_\zeta + E_E + E_H \qquad (1)$$

where E_I is the input energy, E_K is the kinetic energy, E_ζ is the damping energy, E_E is the elastic strain energy, and E_H is the hysteretic energy (e.g Uang and Bertero, 1988). Typical limitation of this approach is that the computed energy is essentially converted to peak relative velocity (Akiyama, 1985), thus using energy merely to compute equivalent relative velocity spectra, and then the classical response spectrum superposition method is used. Further the effects of soil-structure interaction are ignored, and therefore significant mechanisms of energy loss (nonlinear response of the soil and radiation damping) are thus neglected, leading to erroneous inferences about the energy available to drive the structural response. Other simplifications and important omissions in equation (1) are that the dynamic instability and the effects of gravity on nonlinear response are usually ignored (Husid, 1967; Lee, 1979; Todorovska and Trifunac 1991, 1993).

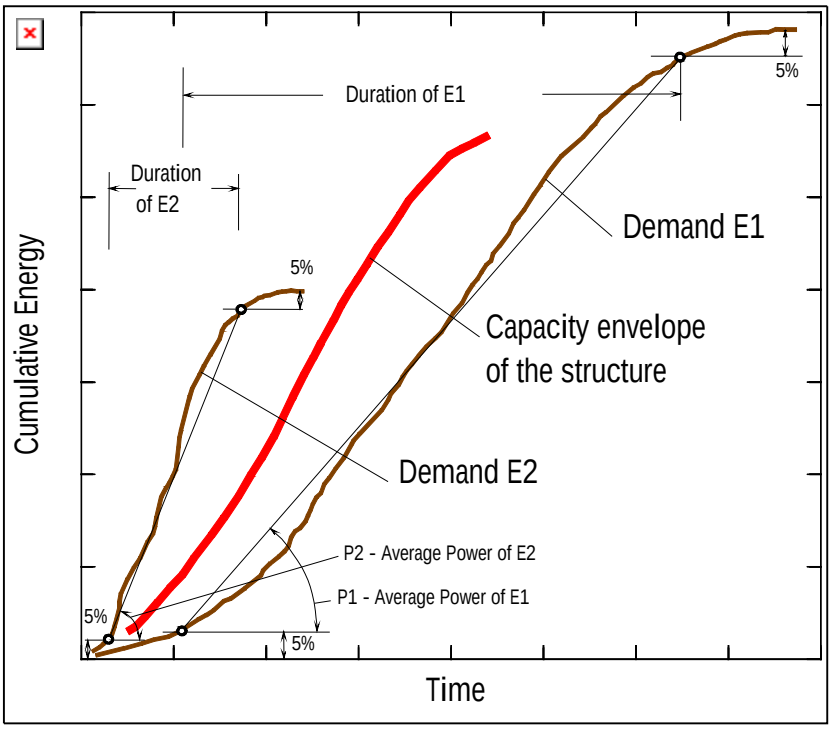

Fig.1 Comparison of strong motion demands E1 and E2 with an envelope of structural capacity.

Fig. 1 illustrates the cumulative wave energies recorded at a building site during two hypothetical earthquakes (demands E1 an E2), and presents the conceptual framework for development of the power design method. E1 results in a larger total shaking energy at the site, and has long duration of shaking leading to relatively small average power, P1. E2 leads to smaller total shaking energy at the site, but has short duration and thus larger power, P2. The power capacity of a structure cannot be described by one unique cumulative curve, as this depends on the time history of shaking. For the purposes of this example, the line labeled "capacity envelope of the

structure" can be thought of as an envelope of all possible cumulative energy paths for the response of this structure. Fig. 1 implies that E1 will not damage this structure, but E2 will. Hence, *for a given*

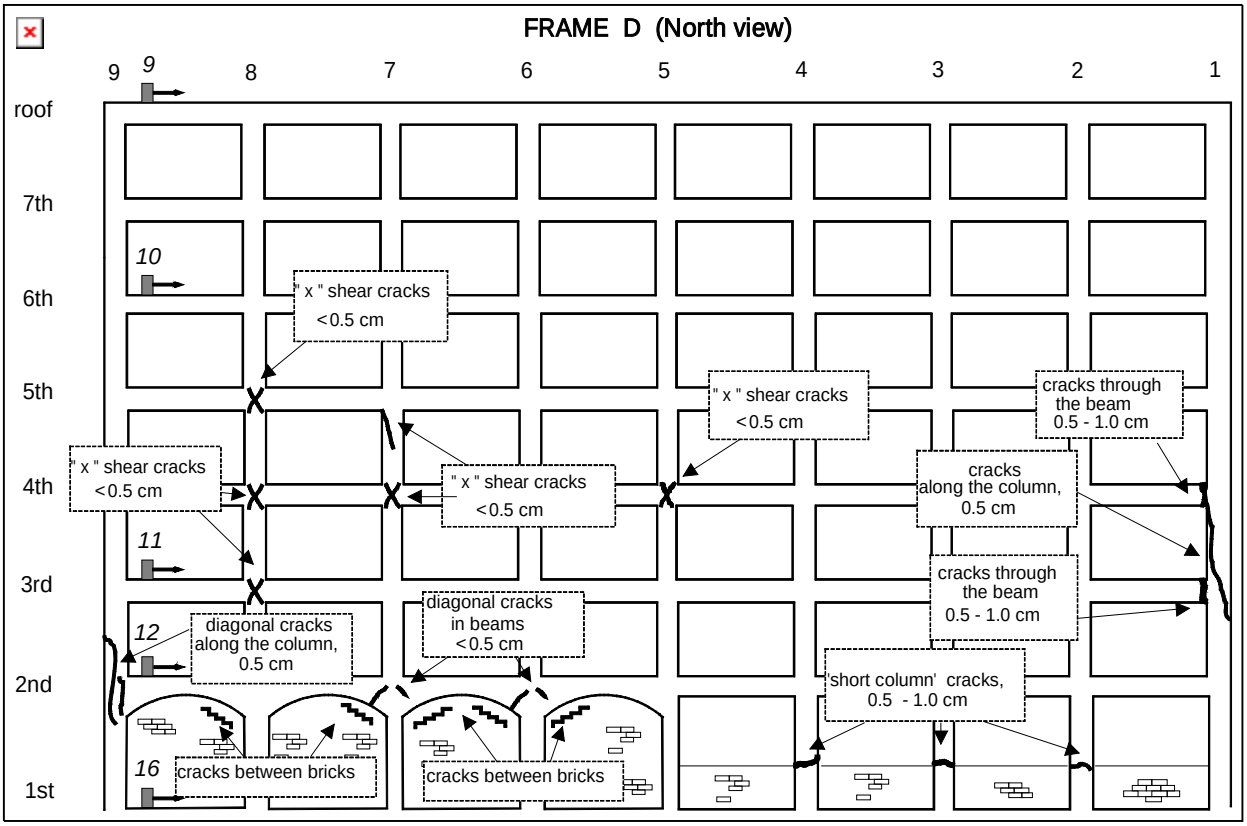

Fig. 2a. Observed Damage of Frame D.

structure, it is not the total energy of an earthquake event (and the equivalent energy compatible relative velocity spectrum), but the rate with which this energy arrives and shakes the structure, that is essential for the design of the required power capacity of the structure to withstand this shaking, and to control the level of damage (Trifunac et al. 2001d).

In this paper elementary aspects of response, based on the energy and power of the wave motion, are illustrated. It will be shown how this power can be compared with the temporal and spatial capacity of the structure to absorb the incident wave energy.

2. CASE STUDY - Van Nuys Hotel (VN7SH)

The example building used in this work is a seven-story hotel (VN7SH) located in Van Nuys, California. It was damaged by the 1994 Northridge, California earthquake (Ivanović et al. 1999a,b, Trifunac and Hao 2001, Trifunac et al. 1999a,b). The building, designed in 1965, and constructed in 1966 (Blume and Assoc. 1973, Mulhern and Maley 1973), is 18.9 × 45.7 m in plan, has seven stories, and is 20 m high. The typical framing consists of four rows of columns spaced on 6.1 m centers in the transverse direction and 5.7 m centers in the longitudinal direction (nine columns). Spandrel beams

surround the perimeter of the structure. Lateral forces in the longitudinal (EW) direction are resisted by interior column-slab frames (B and C), and exterior column spandrel beam frames (A and D). The added stiffness in the exterior frames associated with the spandrel beams creates exterior frames that are roughly twice as stiff as interior frames. The floor system is reinforced concrete flat slab, 25.4 cm

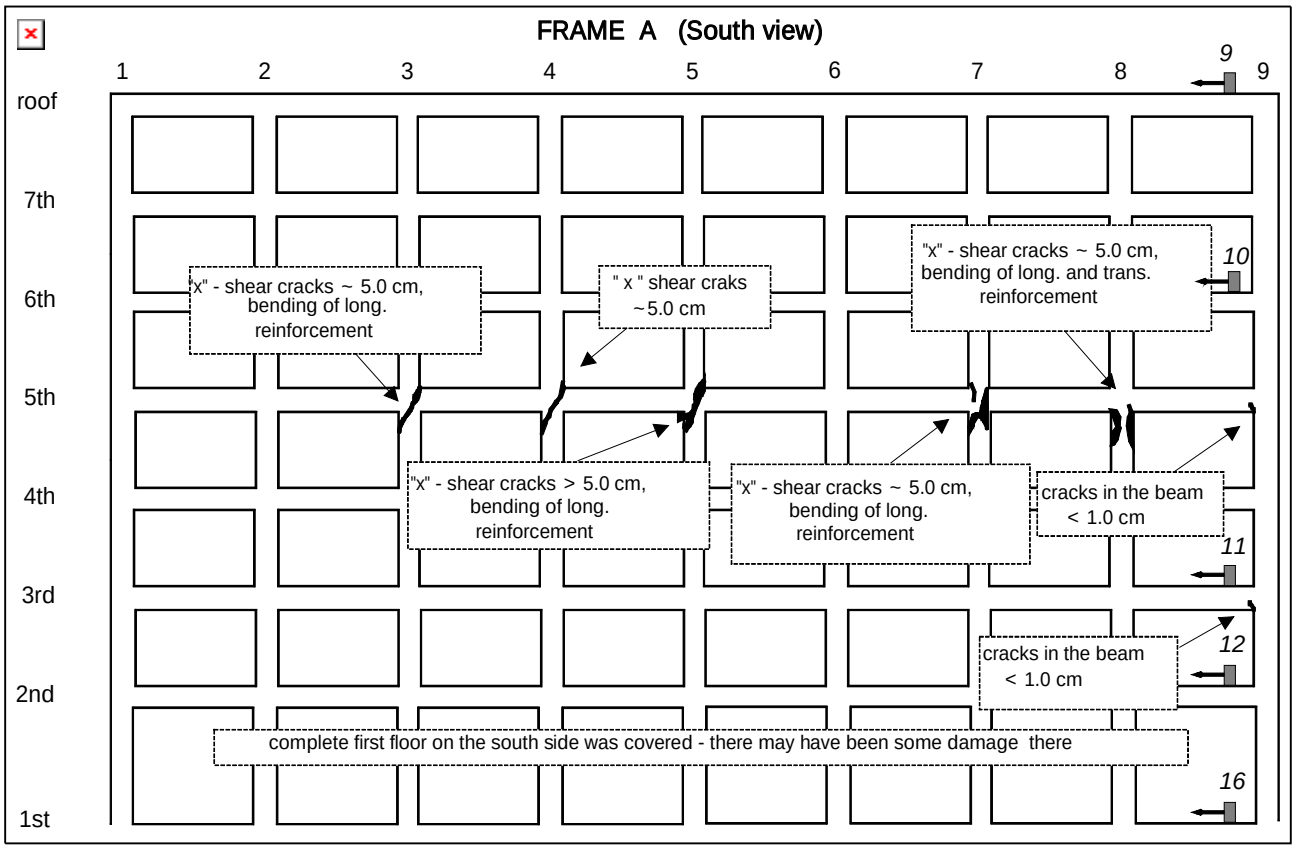

Fig. 2b. Observed Damage of Frame A.

thick at the second floor, 21.6 cm thick at the third to seventh floors, and 20.3 cm thick at the roof (Browning et al. 2000, De La Llera at al. 2001, Islam 1996, Li and Jirsa 1998, Trifunac and Ivanović 2003).The building is situated on undifferentiated Holocene alluvium, uncemented and unconsolidated, with a thickness of < 30 m, and an age of < 10,000 years (Trifunac and Todorovska 1998b). The average shear-wave velocity in the top 30 m of soil is 300 m/s, and the soil-boring log shows that the underlying soil consists primarily of fine sandy silts and silty fine sands. The foundation system consists of 96.5-cm deep pile caps, supported by groups of two to four poured-in-place 61-cm-diameter reinforced concrete friction piles. These are centered under the main building columns. All of the pile caps are connected by a grid of beams. Each pile is approximately 12.2 m long and has a design capacity of over 444.82×10^3 N vertical load and up to 88.96×10^3 N lateral load. The structure is constructed of normal-weight reinforced concrete (Blume and Assoc. 1973).

Earthquake Damage. The $M_L = 6.4$ Northridge earthquake of January 17, 1994 severely damaged the building. The structural damage was extensive in the exterior north (D) (Fig. 2a) and south (A) (Fig. 2b) frames that were designed to take most of the lateral load in the longitudinal (EW) direction.

Severe shear cracks occurred at the middle columns of frame A, near the contact with the spandrel beam of the 5th floor (Fig. 2b). Those cracks significantly decreased the axial, moment, and shear capacity of the columns. The shear cracks that appeared in the north (D) frame (Fig. 2a) caused minor to moderate changes in the capacities of these structural elements. No major damage to the interior longitudinal (B and C) frames was observed, and there was no visible damage to the slabs or around the foundation. The nonstructural damage was significant. Photographs and detailed descriptions of the damage from the earthquake can be found in Trifunac et al. (1999b) and Trifunac and Hao (2001). Analysis of the relationship between the observed damage and the changes in equivalent vertical shear-wave velocity in the building can be found in Ivanović et al. (1999b), and Todorovska and Trifunac (2006d). A discussion of the extent to which this damage has contributed to the changes in the apparent period of the soil-structure system can be found in Trifunac et al. (2001a,b).

Strong-Motion Records. The EW response of VN7SH was recorded by a 13-channel CR-1 central

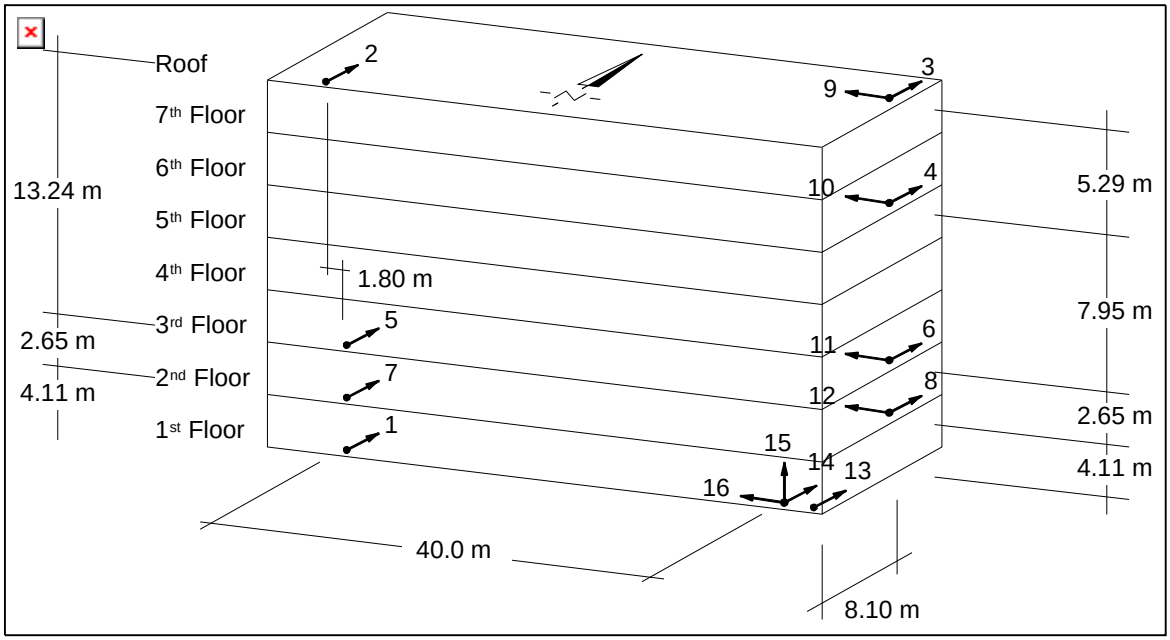

Fig. 3. Location of CR-1 channels (1-13), and of SMA-1 accelerograph (14-16).

recording system and by one tri-component SMA-1 accelerograph (Fig. 3), with an independent recording system, but with common trigger time with the CR-1 recorder (Trifunac et al. 1999b). The five transducers, which recorded EW response of the building during earthquake, were located at Ground (first), second, third, and sixth floors and on the Roof (Fig. 2a,b; 3).

2.1 Previous work

Two full-scale ambient vibration tests of VN7SH were performed (Ivanović et al., 1999a; 2000) following the earthquake. During the second ambient vibration survey, measurements of wave

motion through the building foundation showed that the foundation is "flexible" and deforms with the passage of micro-tremor waves, which indicated that for studies of soil-structure interaction the rigid foundation assumption may not be appropriate (Trifunac et al., 1999a). The apparent period of the soil-structure system and its dependence upon the response amplitudes in VN7SH were described by Trifunac et al. (2001a,b), and an application of off-line and on-line identification techniques to the building response data in VN7SH was presented by Loh and Lin (1996). A continuum mechanics representation of VN7SH in terms of isotropic and anisotropic two-dimensional models and their response to incident wave motion was considered by Todorovska et al. (2001a,b). The feasibility of identifying the observed damage through wave propagation studies using recorded earthquake responses was explored in Ivanović et al. (1999b), Trifunac et al. (2003), and Todorovska and Trifunac (2006).

The engineering studies of VN7SH have focused mainly on its longitudinal (EW) response. Without exception, these studies have neglected the effect of soil-structure interaction and have implicitly assumed that all non-linearities in the observed response are associated with the building structure.

Islam (1996) considered two two-dimensional models for EW response of the building. Assuming the building to be fixed at the ground floor level, he used the triangular distributed horizontal load to perform a push-over analysis. Fig. 4 shows his results for V/W, the resulting base shear (V), normalized by the appropriate fraction of building weight (W), versus roof displacement, assuming that the south perimeter frame (A) resists one third of the lateral load. Islam concluded that "many of the structural elements may have exceeded their elastic limit state at approximately 4 seconds into the earthquake. However, the most severe damage—e.g., breakdown of the entire load path in the south perimeter frame columns immediately below the 5th floor level—may have actually occurred at approximately 9 seconds, which coincides with the time of the peak ground acceleration in the longitudinal direction." He also notes that "a push-over analysis performed on the longitudinal frame with a triangular load pattern was unable to predict the damage observed in the building."

Li and Jirsa (1998) performed a *non-linear time history* analysis of VN7SH in the longitudinal (EW) direction "only because most of the damage occurred in this direction." Acceleration time histories recorded at ground level were used as input ground motion, and columns were assumed to be fixed at the base. Soil-structure interaction was not included in the models. Effective stiffness and residual lateral capacity were chosen so that the period of calculated response-time history would match the recorded time history, and 0.35 EI_g was chosen as an effective stiffness for all beams and columns. Their analysis was two-dimensional, and therefore no torsional effects of excitation and of response could be included. Li and Jirsa stated that "Push-over analysis

successfully predicted that the structure almost lost its lateral load-resisting capacity, and the shear

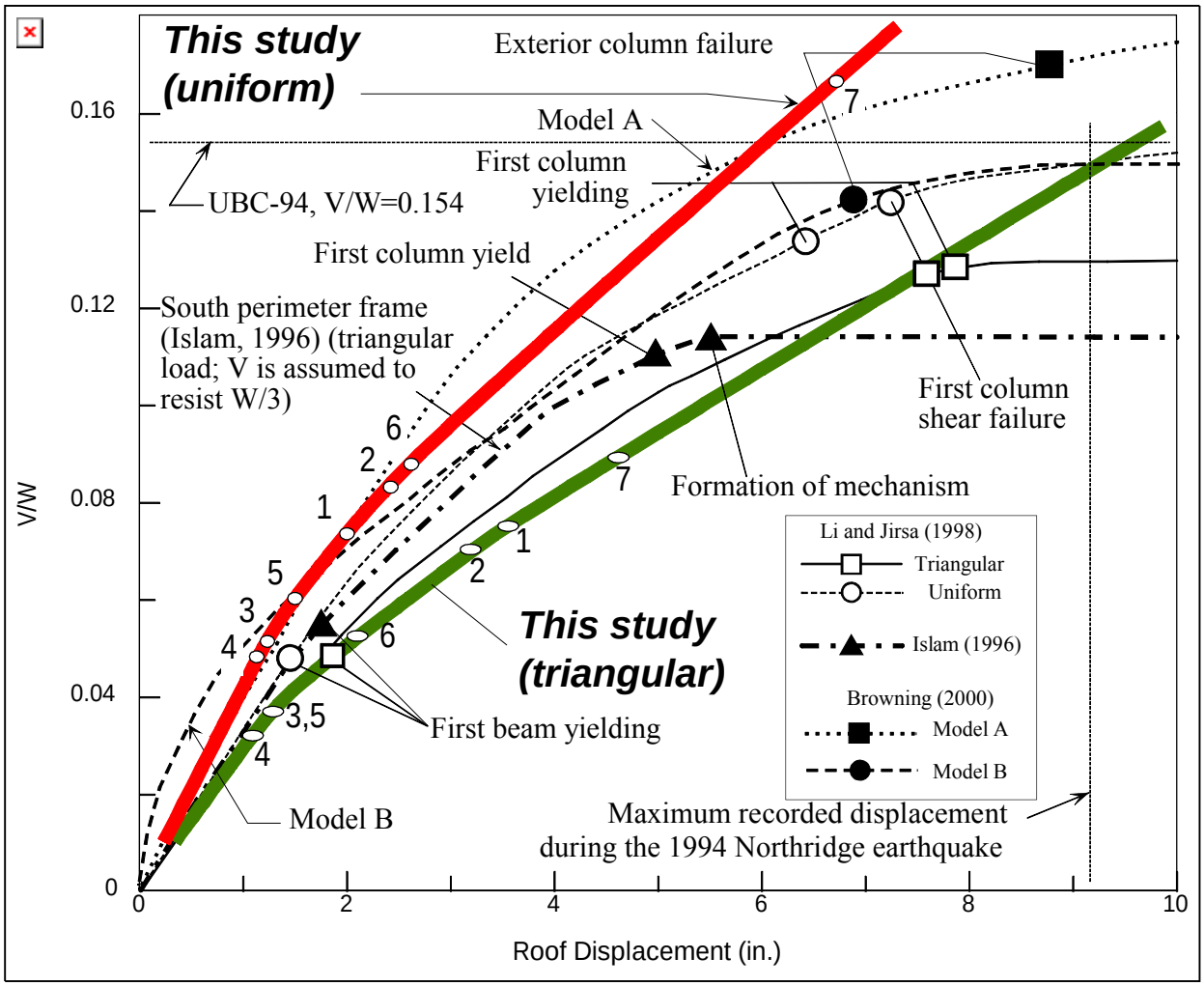

Fig. 4. Base shear (V) coefficient normalized by total building weight, W, versus EW roof displacement of VN7SH (*This study – open circles indicate first occurrence of nonlinear strain, at floors 1 through 7;* Islam, 1996; Li and Jirsa, 1998; and Browning et al, 2000: Models A and B).

failures of columns occurred prior to reaching the maximum roof displacement the building experienced during the earthquake."

Browning et al. (2000) compared three independent analyses, including their own results, with regard to the response of VN7SH to the Northridge earthquake: Approach A (by Lynn and Moehle); Approach B (by Browning and Sozen); and Approach C (by Li and Jirsa). Because approach C has already been summarized, we mention briefly only the results of the analyses based on approaches A and B. ***Approach A*** idealizes the building as a two-dimensional frame and considers only longitudinal (interior and exterior) framing lines. A simple bi-linear relation without stiffness or strength degradation is used to describe load deformation properties of the

frames. The foundation is assumed to be rigid—that is, no soil-structure interaction is considered, and the authors used triangular load distribution with monotonically increasing amplitude in their push-over analysis (Fig. 4). Dynamic *non-linear response histories* were computed for the motion measured at the base of the building. ***Approach B*** used a model geometry similar to that of model A, but the in-fill walls were assumed not to contribute to resistance to the lateral forces. A *Takeda non-linear model* with unloading stiffness reduction equal to 0.4 was adopted, and non-linear static and dynamic response analyses were conducted. The results of the push-over analysis are shown in Fig. 4.

De la Llera et al. (2002) noted that "planar analyses of the building reported previously are obviously not capable of predicting… torsional motion." They developed an idealization of the building consisting of a "single column-like element" (SEM) connecting two consecutive floors and used this model to interpret the three-dimensional response of the VN7SH building to the earthquake. As in all previous investigations of the response of this building, De la Llera et al. (2001) ignored soil-structure interaction effects in their analyses of translational and torsional responses.

3. NONLINEAR WAVES

Wave propagation models of buildings have been used for many years (Kanai, 1965), but are only recently beginning to be verified against observations (Ivanovic et al. 1999b; Todorovska et al.,

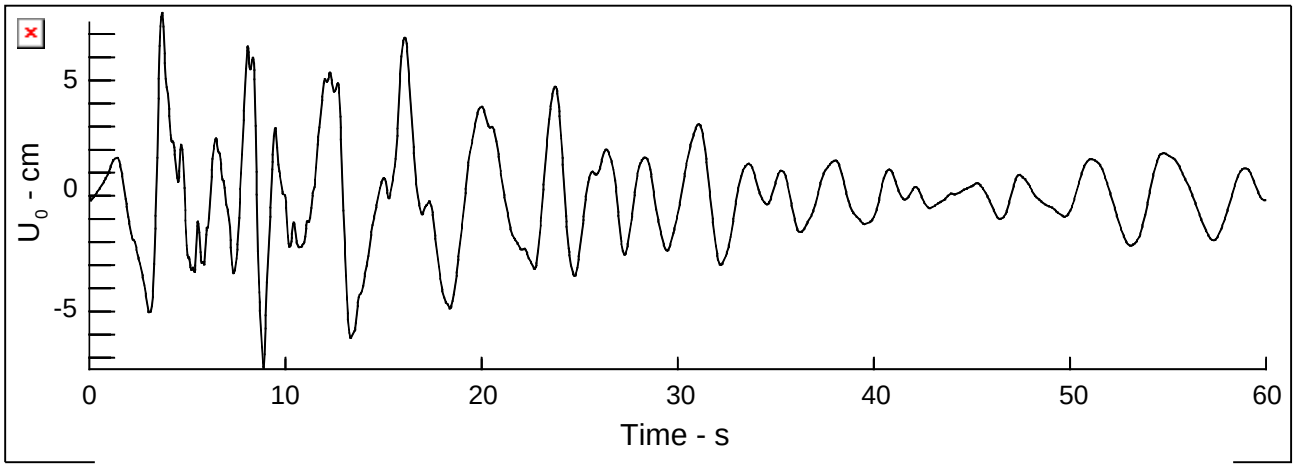

Fig. 5. Incident Ground Motion

2001a,b,c; Trifunac and Todorovska, 2001; Trifunac et al., 2001d). Continuous, 2-D wave propagation models (homogeneous, horizontally layered and vertically layered shear plates) can be employed to study the effects of traveling waves on the response of long buildings (Todorovska et al., 1988; Todorovska and Trifunac, 1989; 1990a,b; Todorovska and Lee, 1989). Discrete-time 1-D wave propagation models were proposed to study the response of tall buildings (Safak, 1998), and 2-D finite difference methods were used to study linear and non-linear soil-structure interaction (Gicev, 2005).

In the following the elementary principles of wave propagation through a layered shear beam model will be used to demonstrate the relationships between the power of incident strong ground motion, and of the building response.

3.1 The building model

We consider a one-dimensional finite difference model, and use the velocity of shear waves and the density of the slabs and inter-story columns based on the analysis of impulse response for EW recorded motions in Holiday Inn hotel (Todorovska and Trifunac 2006d). These parameters together with the inter-story heights as adopted in this study are summarized in Table 1. As can be seen from this table, the stiffness and the density of the floors is much larger than the stiffness of the columns. Therefore it can be expected that the floors will move essentially as rigid bodies. The yielding and the nonlinear characteristics of the material, have been estimated previously from the East-West response of this model, by assuming that the input ground motion can be approximated by strong motion recorded at the first (ground) floor (channel 16). We did this by comparing the computed motions with the recorded motions at higher floors in the building (channel 12 at the second floor, channel 11 at the third floor, channel 10 at the sixth floor, and channel 9 at the roof) (Gicev and Trifunac, 2006b). The location of the instruments in the building, which recorded EW response, is shown in Fig. 3. By varying the yielding strain and the strengthening factor γ, assuming that they are the same for whole building, and minimizing the error between the recorded and the calculated responses, we obtained the best estimates for the yielding strain $\varepsilon_y = 0.0025$ and for $\gamma = 0.44$. These two parameters together with those in Table 1 then complete the description of our finite difference bilinear model parameters (Gicev and Trifunac 2006b).

Table 1. One-dimensional building model.

	Interstory Height $h_{interstosry}$ (m)	Slab Thickness h_{slab} (m)	$\beta_{interstory}$ (m/s)	β_{slab} (m/s)	$\rho_{interstory}$ (kg/m^3)	ρ_{slab} (kg/m^3)
Roof slab		0.203		2000		2384
Seventh story	2.44		73.15		82.90	
Seventh floor slab		0.215		2000		2384
Sixth story	2.44		76.20		82.90	
Sixth floor slab		0.216		2000		2384
Fifth story	2.44		77.72		82.90	
Fifth floor slab		0.216		2000		2384
Fourth story	2.44		79.25		82.90	
Fourth floor slab		0.216		2000		2384
Third story	2.44		91.44		82.90	
Third floor slab		0.216		2000		2384
Second story	2.44		129.50		82.90	
Second floor slab		0.254		2000		2384
First story	3.86		140.20		76.92	

In this paper, we adopt these same model parameters, but consider the one-dimensional interaction between the soil and the building by taking two more spatial points in the soil (Gicev and Trifunac 2006a). We further assume that the soil is linear having shear wave velocity $\beta_s = 300\,\mathrm{m/s}$ and density $\rho_s = 2000\,\mathrm{kg/m^3}$. We assume that the horizontal wave motion in the ground propagates upward and it is the one recorded at channel 16 (Fig.5). Of course, this is not the actual incident wave motion during the Northridge main event, because the record in channel 16 resulted from the incident and reflected wave field at the base of the building. Also this record contains the soil-structure interaction effects. Nevertheless, using this record as an approximation for the arriving waves in the ground we can study the overall features of the response of the building during the main event of Northridge earthquake from energy point of view, approximately. In all other respects our modeling of the building by one-dimensional finite difference model is identical to the one described in Gicev and Trifunac (2006a), and its description is therefore not repeated here.

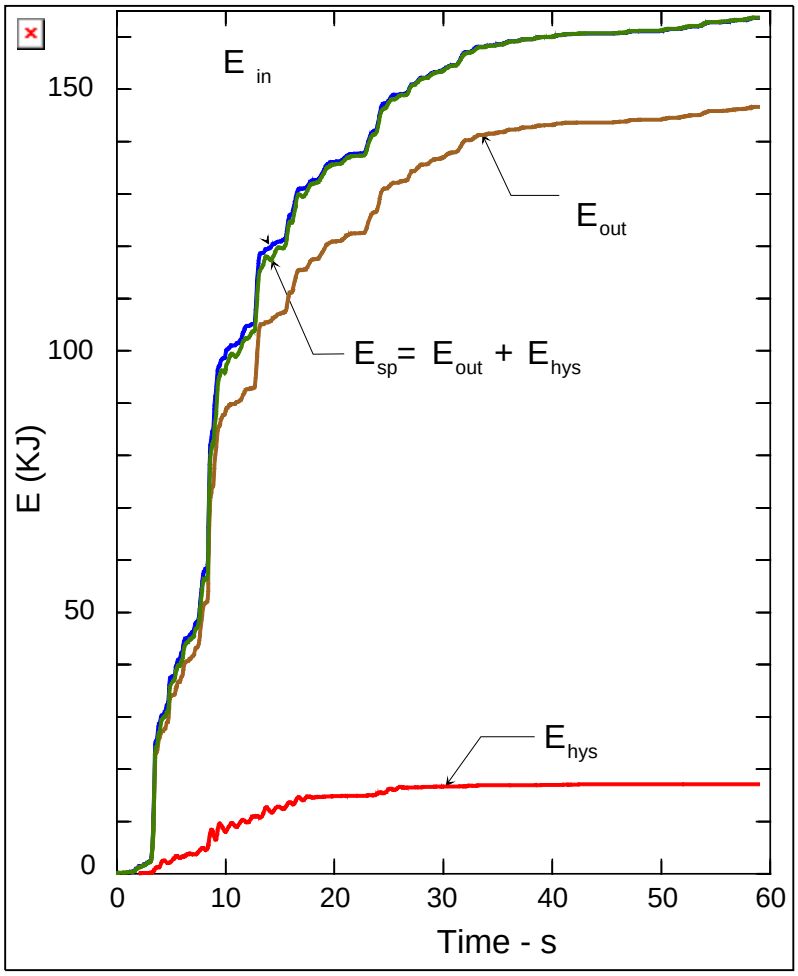

Fig. 6. Energy distribution in VN7SH, during the Northridge Earthquake. The spent energy consisting of energy going out of the building and the spent hysteretic energy, balance the input energy.

3.2 Results

3.2.1 Energy distribution in the model

Because the model we study represents a conservative system, the kinetic and elastic part of potential energies, the energy radiated out from the building into the soil, and the energy spent for development of the permanent strains in the building, must add up to the incident wave energy. In Fig. 6 the energy radiated out of the building into the soil E_{out}, and the energy spent on the work leading to

permanent strains, E_{hys} are shown versus time. The energy is computed in kilojoules ($1\,\mathrm{KJ} = 1\,\mathrm{KN}\cdot\mathrm{m}$), while the time is shown in seconds.

The input energy, $\mathrm{E_{in}}$, is computed from the input displacement record (Fig. 5). First, by differentiation of the displacement record with respect to time, the input particle velocity is obtained. The input energy, assuming that the cross section of the model is $\mathrm{A} = 1\mathrm{m}^2$, is computed assuming vertically propagating one-dimensional plane waves,

$$E_{in} = \rho_s \cdot \beta_s \int_0^T v^2 dt \cong \rho_s \cdot \beta_s \cdot \sum_{k=1}^{M} v_k^2 \cdot \Delta t \qquad (2)$$

where ρ_s and β_s are the density and the shear wave velocity of the soil, $\mathrm{v} = \frac{\partial \mathrm{u}_0}{\partial \mathrm{t}}$ is the input particle velocity, T is the time at the end of the record, k is the order number of a time step, $\mathrm{M} = \frac{\mathrm{T}}{\Delta \mathrm{t}}$ is the discrete time at the end of the record and $\mathrm{v_k} = \frac{\mathrm{u_{0,k}} - \mathrm{u_{0,k-1}}}{\Delta \mathrm{t}}$ for $\mathrm{k} > 1$, and $\mathrm{v_1} = \frac{\mathrm{u_{0,1}}}{\Delta \mathrm{t}}$ for $\mathrm{k} = 1$, are the discrete particle velocities.

The output energy, $\mathrm{E_{out}}$, is computed from the velocity of the wave going downward, v_{out}, (Gicev and Trifunac 2006a). The cumulative output energy is then computed as

$$E_{out} = \rho_s \cdot \beta_s \int_0^T v^2 dt \cong \rho_s \cdot \beta_s \cdot \sum_{k=1}^{M} \left(v_{out}^k\right)^2 \cdot \Delta t \qquad (3)$$

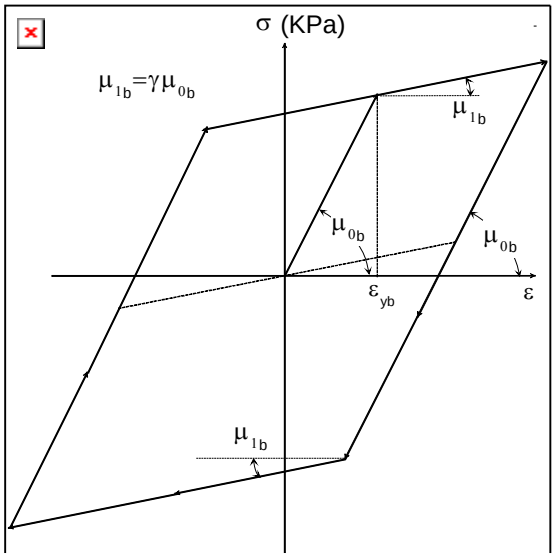

Fig. 7. Hysteresis loop representing $\sigma(\varepsilon)$ during time $T_{0.i} < t < T_{0.i+1}$.

The hysteretic energy, $\mathrm{E_{hys}}$, is the energy spent on the development of permanent strains in the building. The hysteretic loop (Fig. 7) represents the relation $\sigma(\varepsilon)$ at a point during one cycle of the response $\mathrm{T_{0,i}} < \mathrm{t} < \mathrm{T_{0,i+1}}$, where $\mathrm{T_{0,1}} = 4 \cdot \sum_{\mathrm{j=1}}^{14} \frac{\mathrm{h_j}}{\beta_\mathrm{j}} \approx 0.8\,\mathrm{sec}$ can be used to approximate the apparent period of the building. Depending upon the input ground motion and the time during strong motion, the loop can be narrower or wider. By adding the areas of those loops, and assuming no strength reduction from repetitive loads, we can compute the energy spent for development of permanent strains at a point. Next, we generalize this for a layer (continuous equivalent representation of the columns

and walls at a given floor), and for the whole building. The hysteretic energy for a certain layer is obtained as sum of the loops at the points belonging to that layer, while the hysteretic energy for whole building is obtained as sum of the energies in all layers. The hysteretic energy in the building in discrete time space is computed as:

$$E_{hys} = \sum_{i=3}^{N} \Delta x_i \cdot \sum_{k=1}^{M} \sigma_{av}^{k} \cdot \Delta\varepsilon^{k} \qquad (4)$$

where the indices i and k stand for spatial and temporal discrete points in the model. N is the point

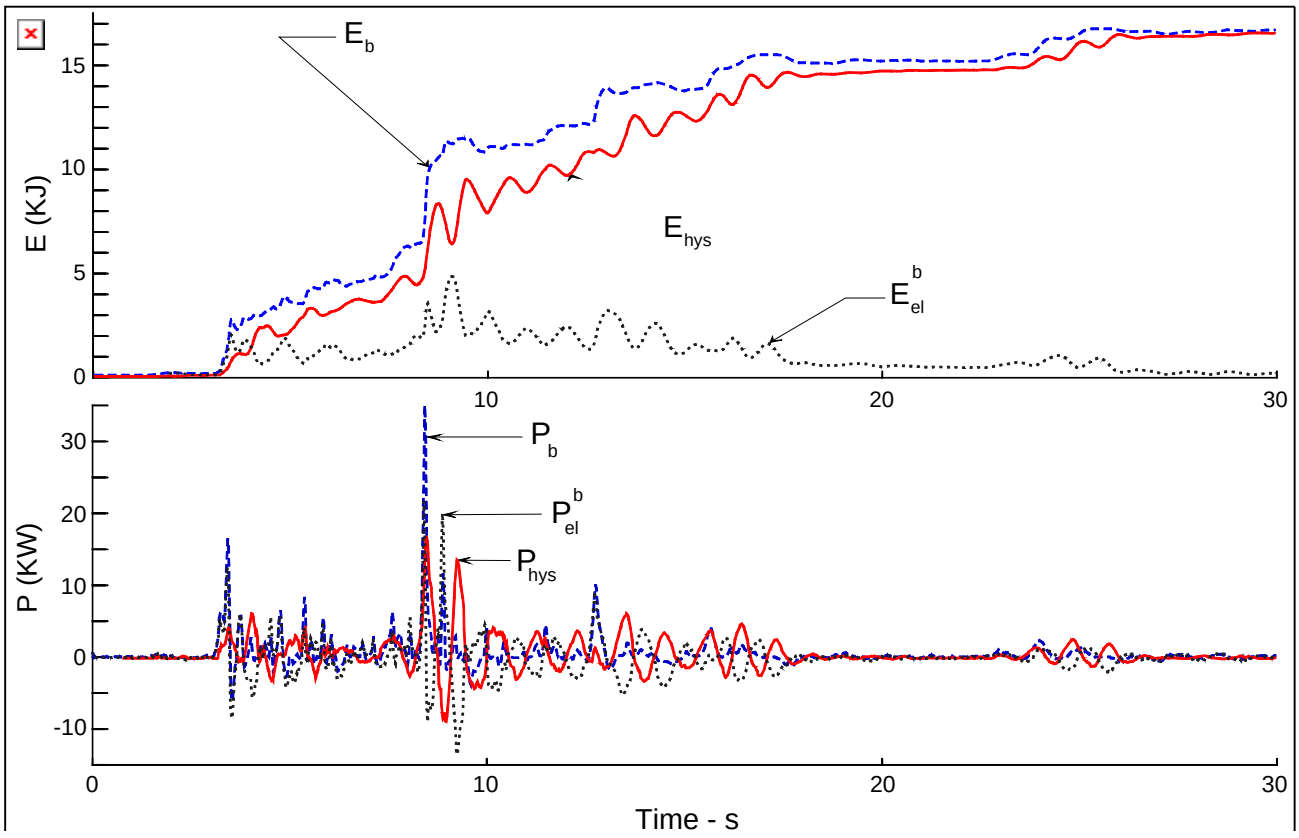

Fig. 8. Energy, E_b (top), and power, P_b (bottom), in the VN7SH building during Northridge earthquake, where $E_{el}^{b} = E_b - E_{hys}$.

representing the top of the building, and M is the point representing the end of the record. $\sigma_{av}^{k} = \dfrac{\sigma^{k} + \sigma^{k-1}}{2}$ is the average stress at a point i in the time step k, and $\Delta\varepsilon^{k}$ is the strain increment at the point i in the k-th time step. The points in the slabs do not contribute to the hysteretic energy, because those are assumed to remain linear and only transmit the wave energy to the layers above and bellow. As can be seen from Fig. 6, after about t = 30 sec, there is negligible growth of all energies, and therefore in the following analysis we consider only the first thirty seconds of strong motion.

Subtracting from the input energy (Eq. (2)) the output (radiated) energy (Eq. (3)) we obtain the instantaneous energy in the building, E_b, (Fig. 8). The difference

$$E_{el}^{b} = E_b - E_{hys} \qquad (5)$$

then represents the instantaneous elastic (linear) energy in the building. All these energies are computed in KJ. In the bottom of Fig.8, the derivatives (power) of these three energies are shown versus time. The power is shown in kilowatts $(1\,\mathrm{KW} = 1\,\mathrm{KJ/s} = 1\,\mathrm{KN}\cdot\mathrm{m/s})$. Until the end of the record, one part of the elastic energy is radiated, contributing to the output energy, E_{out}, and one part is later spent for development of permanent strains contributing to the hysteretic energy, E_{hys}. A part of the energy in the building is reversible. During loading a fraction of the elastic energy transforms into hysteretic energy, and vice versa, during unloading, a part of hysteretic energy is converted back into elastic energy.

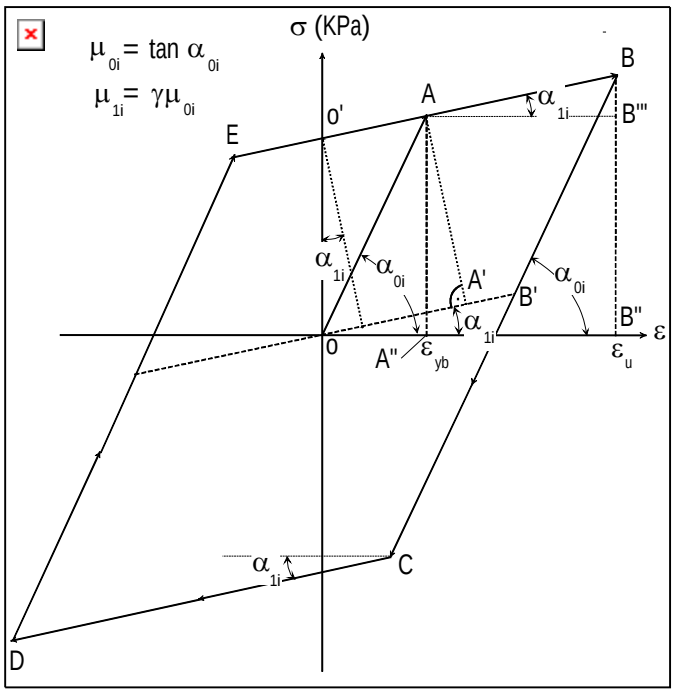

Fig. 9. Hysteresis loop, at strain ε_u, during one period of response.

3.2.2 Energy and power capacities and demands in the building

To study how the VN7SH building performed during Northridge earthquake, we consider the energy and the power capacities of different floors. To determine the energy capacity for one period, E_{T_0}, we consider the hysteretic loop at a point, during which the point reaches the strain, ε_u (Fig. 9). The area of the loop A_i is the energy capacity of the floor i, for that ε_u and per one period

$$A_i = E_{T_0}^{i} = 4 \cdot A_{OABB'} = 4 \cdot \overline{OB'} \cdot \overline{AA'} \cdot h_i . \quad (6)$$

where h_i is the height of the i-th floor. From Fig. 9 there follows

$$\overline{AA'} = \left(\mu_{0i}\varepsilon_{yb} - \mu_{1i}\varepsilon_{yb}\right)\cdot\cos\alpha_{1i}, \quad \text{and} \quad \overline{OB'} = \frac{\varepsilon_u - \varepsilon_{yb}}{\cos\alpha_{1i}} \qquad (7)$$

where $\mu_{1i} = \gamma\mu_{oi}$, and the ductility is

$$d = \frac{\varepsilon_u}{\varepsilon_{yb}}. \qquad (7a)$$

Combining Eq. (7) in Eq. (6) the energy capacity of the floor i per one cycle becomes

$$E^i_{T_0} = 4 \cdot \mu_{0i} \cdot \varepsilon^2_{yb} \cdot (1-\gamma) \cdot (d-1) \qquad (8)$$

While energy capacity per one cycle gives information about the capacity of the floor for oscillatory loading, the energy capacity of the floor i during one quarter period, E^i_q, gives information about the resistance of the floor during a single monotonic loading. From Fig. 9 this energy corresponds to the area of $\overline{OABB''}$ consisting of two triangles and one rectangle

$$A_{OABB''} = A_{OAA''} + A_{A''AB'''B''} + A_{ABB'''} \quad . \qquad (9)$$

From Fig. 9

$$E^i_q = \left[\frac{\mu_{0i}\varepsilon^2_{yb}}{2} + \mu_{0i}\varepsilon_{yb} \cdot (\varepsilon_u - \varepsilon_{yb}) + \frac{\gamma \cdot \mu_{0i} \cdot (\varepsilon_u - \varepsilon_{yb})^2}{2} \right] \cdot h_i \qquad (10)$$

and using $\varepsilon_u = d \cdot \varepsilon_{yb}$ we obtain

$$E^i_q = \frac{\mu_{0i} \cdot \varepsilon^2_{yb}}{2} \cdot \left[1 + 2(d-1) + \gamma \cdot (d-1)^2 \right] \quad . \qquad (11)$$

The energy capacity of the whole building is the sum of the energy capacities of the inter-story layers,

$$E^b_{T_0} = \sum_i E^i_{T_0} \quad i = 1,3,5,\ldots,13 \qquad (12)$$

$$E^b_q = \sum_i E^i_q \quad i = 1,3,5,\ldots,13 \quad . \qquad (13)$$

The power is the derivative of energy with respect to time. We compute the power capacity per full cycle by dividing (8) by the period of the building, T_0, and the power capacity for quarter cycle by dividing (11) by $T_0 / 4$

$$P^i_{T_0} = 4 \cdot \mu_{0i} \cdot \varepsilon^2_{yb} \cdot (1-\gamma) \cdot (d-1) / T_0 \qquad (8a)$$

$$P_q^i = 2\mu_{0i} \cdot \varepsilon_{yb}^2 \cdot \left[1 + 2(d-1) + \gamma \cdot (d-1)^2\right] / T_0 \qquad (11a)$$

From Eqs. (8a) and (11a) it can be seen that the power capacity for one full period is linearly dependent upon the ductility, d, while the power capacity for one quarter period (loading only) depends upon the square of the ductility. The dependence of the power capacity of the building on its ductility is illustrated in Fig. 10. In Fig. 11 the cumulative growths of normalized hysteretic energies in time for each floor and for the whole building are shown.

Trifunac et al. (2001d) estimated the input velocity in the building for equivalent SDOF system that will cause failure, by equalizing the input power in the building and its apparent (based on actual observation of earthquake effects) power capacity. Following this approach, to understand failure, we may compare the maximum power in the floor (building) with the power capacity of the floor (building). In Fig. 11 the cumulative hysteretic energies, during the Northridge earthquake, for all inter-story layers are presented during the first thirty seconds of strong motion, normalized (divided) by the energy capacities for the ductility d = 10. The cumulative energy capacities can be approximated by straight lines, computed from Eq. (8), as

$$E_{cT_0}^i(t) = E_{T_0}^i \cdot \frac{t}{T_0} \qquad (14)$$

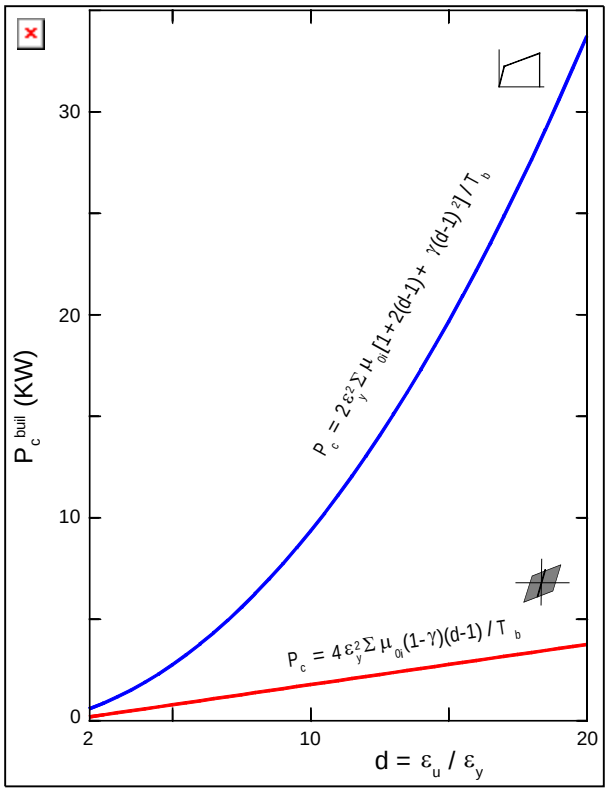

Fig. 10 Power capacities for VN7SH for one whole and one quarter periods.

Table 2 Peak ductilities, $|d|_{max}$, computed by Gicev and Trifunac (2006b).

Inter-story layer i	$\|d\|_{max}$
1	4.10
2	3.67
3	8.64
4	9.39
5	9.39
6	6.73
7	3.71

where t is the time when the energy capacity for full period of the i-th column is computed, and T_0 is the period of the building. The approximation by Eq. (14) is a straight line, with slope $\frac{E_{T_0}^i}{T_0}$, which represents the power capacity for a full cycle of response. Fig. 11 then shows the evolution of the process at each floor. For small oscillations in the beginning of strong motion, the power demand is small and the maximum capacity of the floors is not

mobilized. With arrival of large strong motion pulses (at about 4 and 9 seconds after the trigger time), large nonlinear deformations occur with $E_{hys} / E_{c(d=10)}$ exceeding 1.0.

The ductility demands for this model of VN7SH have been calculated by Gicev and Trifunac (2006b), for different floors, and are summarized in Table 2. The maximum strains occurred during time interval $8.5\text{s} \le t \le 9.5\text{s}$.

From Fig. 11 it can be seen that the cumulative hysteretic energies $E_{hys}(t)$ (see Eq. (4)), normalized with respect to the energy capacities $E_c(t)$ (see Eq. (14)), for ductility d = 10, for example, are in good agreement with the previously computed maximum ductilities for the same building, and for the same excitation, shown in Table 2 (Gicev and Trifunac 2006b).

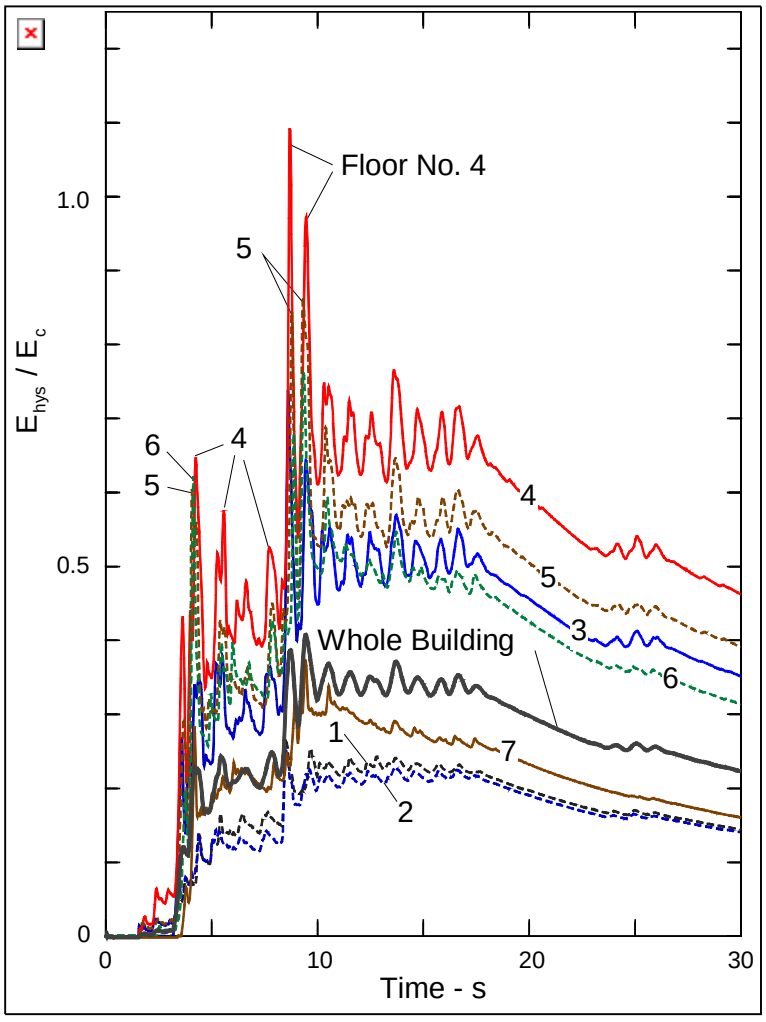

Fig. 11. Normalized cumulative hysteretic energies E_{hys} / E_c, versus time, in seven layers (floors), and in the whole building.

The hysteretic energy demand takes into account only the strains, but does not consider the time rates of change of those strains. In contrast, the power takes into account the energy rates in time, which we compute as derivatives of the energy, normalized by the rates representing capacity for one hysteretic cycle (per time T_0 for P_{T0}), or normalized by the rates representing capacity for one monotonic loading interval (per time $T_0 / 4$ for P_q).

Fig. 11 shows that at the fourth and the fifth floors, the hysteretic energy, starting from t = 4 s, becomes larger than the energy capacity E_c for d ~ 5, while it exceeds the energy capacity for d = 10 only in short interval around t = 9 s. The energy demand for the whole building is slightly higher than the energy capacity for d ~3.5 in the interval 8.5s < t < 20s.

Figs. 12a,b show more detailed view of the physical nature of the demands and of capacities, for two time windows, from 3 to 6 and from 8 to 11 seconds, in terms of relative power. In these figures the relative power is plotted, in terms of the ratio of P_{hys}, which is the time rate of change of E_{hys} (see Eq. (4)), normalized (divided) by $P_{c,quart}$ (see Eq. (11a)), and calculated for d=10. It is seen that this power ratio approaches 2 at the 4-th and at the 7-th floor, while at the 5-th and at the 6-th floors it is near 3 around 4 seconds. At the 3-rd, 4-th, 5-th and 6-th floors, this ratio exceeds 1 around 5.2 seconds. The same ratio exceeds 5, for example, at 3-rd, 4-th, 5-th, and 6-th floors, between 8.5 and 8.8 seconds, and again at the 5-th floor, around 9.2 seconds. The largest peak of the ratio $P_{hys} / P_{c,quart}(d = 10)$ occurred on the 4-th floor, with amplitude larger than 8, at about 8.6 seconds. These results are in excellent agreement with the location of the observed post earthquake damage on the same floor (Figs. 2a,b), and with the analyses of the peak strains and peak drifts in the response of the one-dimensional model of VN7SH to Northridge earthquake (Gicev and Trifunac 2006b).

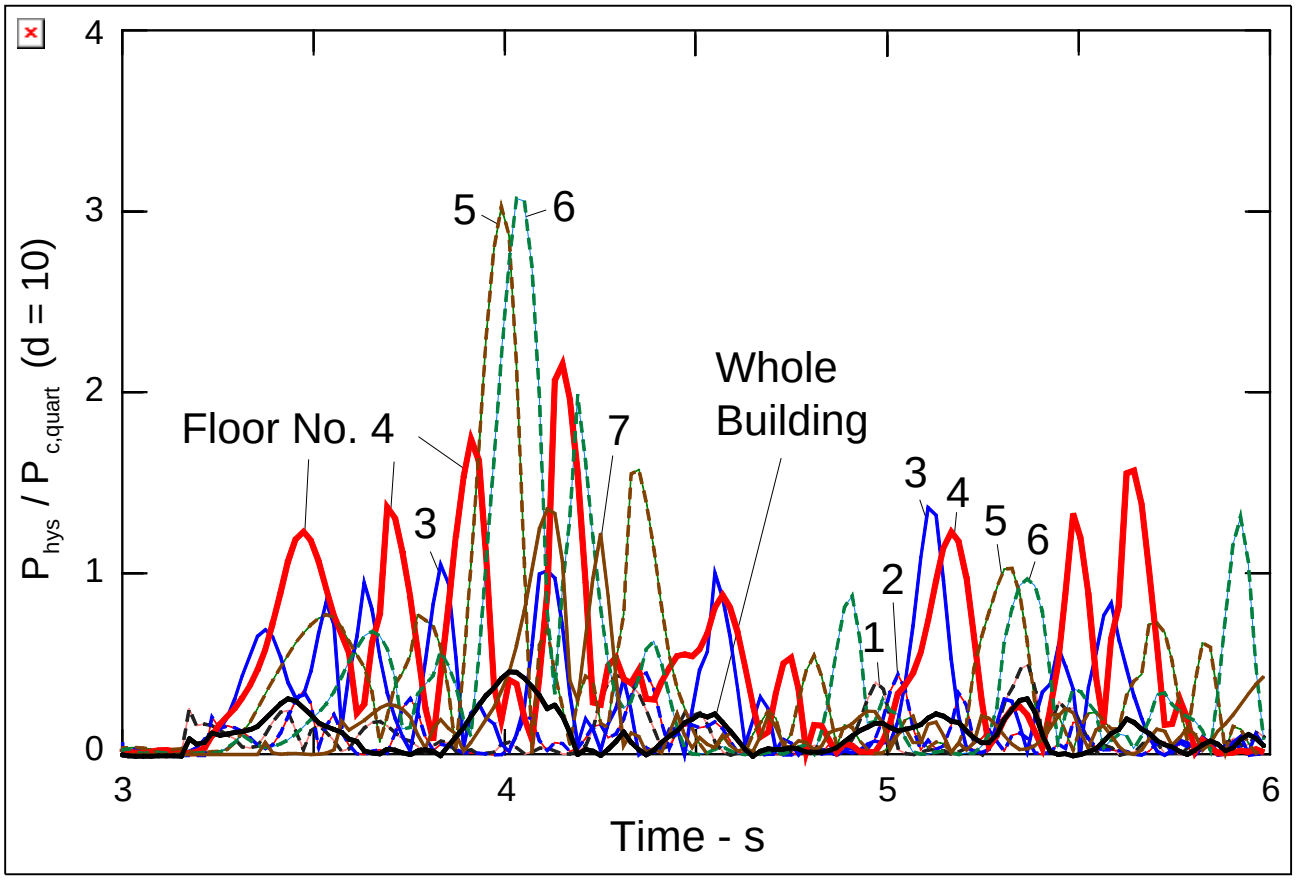

Fig. 12a. Normalized power demands in the model of VN7SH building, during excitation by Northridge earthquake, shown separately at seven floors, and in the whole building, for $3 < t < 6$ s.

Further perusal of the largest peaks of the power ratios, $P_{hys} / P_{c,quart}(d = 10)$ (Figs. 12a,b), will show that those occur in sequence, at progressively higher floors, and at the times following the entrance of the strong pulses from the ground motion into the building. The local peak ratios occur in Fig. 12a around 4 s (at floors 3, 4, 5, and 6), around 5.2 s (at floors 1, 2, 3, 4, 5 and 6), and in Fig. 12b around 8.4 s (at floors 1, 2, 3, 4, 5, and 6), 9.3 s (at floors 4, 5 and 6), and 10.3 s (at floors 3, 4, 5, 6 and 7). As they propagated up into the building, these power pulses caused damage along their path, whenever

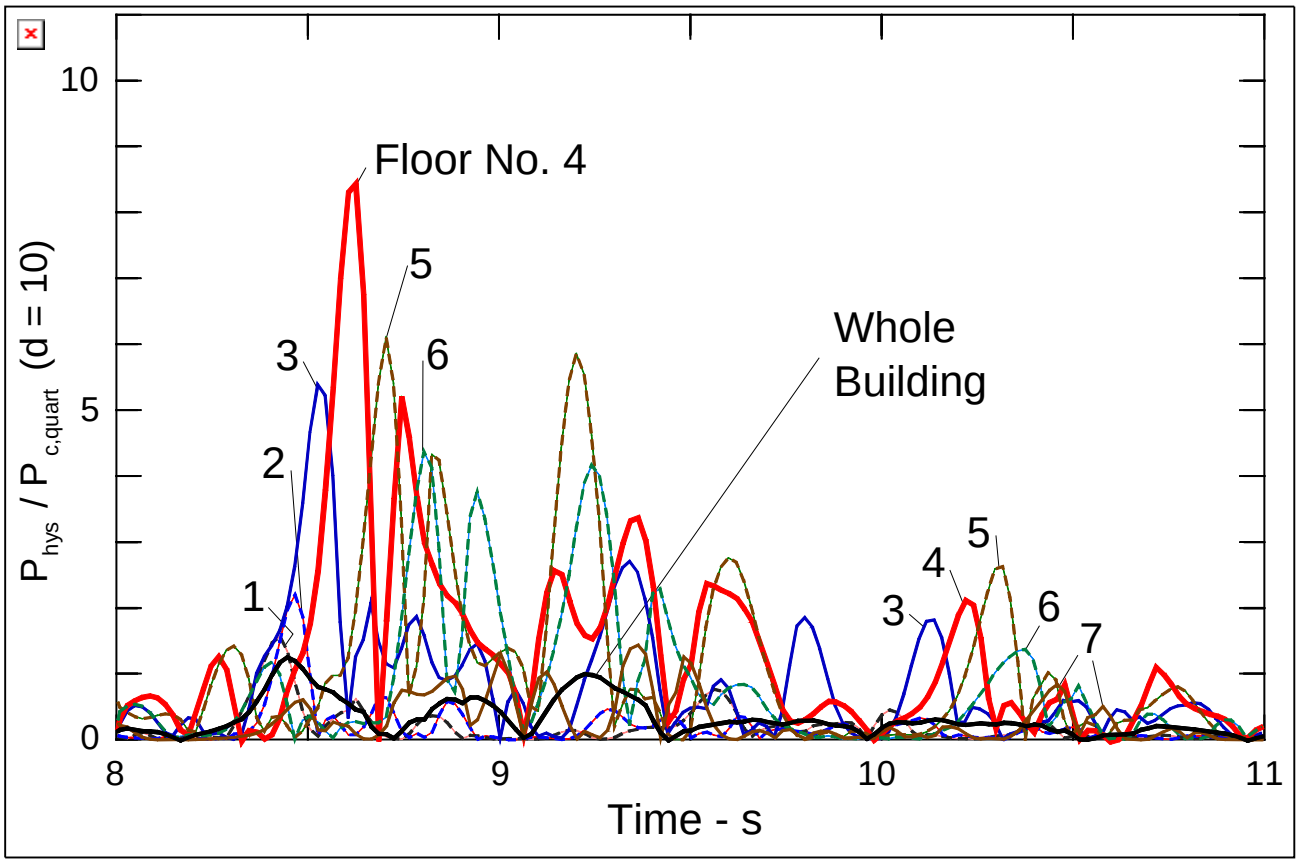

Fig. 12b. Normalized power demands in the model of VN7SH building, during excitation by Northridge earthquake, shown separately at seven floors, and in the whole building, for $8 < t < 11$ s

and wherever the power ratio exceeded the value of about 2. From the time delays between these consecutive pulses in Figs 12a,b, we can estimate the average wave speeds associated with the propagation of their energies. Around 4 s and 5 s (in Fig.12a) this speed is about 40 m/s. Around 8.5 s, and 10.2 s (in Fig. 12b) this speed is lower, about 30 m/s. Comparing these speeds with the initial (linear) velocities in our model (Table 1), which are in the range from 73 m/s (seventh story), to 91 m/s (third story), to 140 m/s (first story), it can be concluded that those lower speeds resulted from nonlinear deformations in the model. Their values and their times of occurrence are consistent with the results of other direct (see Table 2 and Fig. 11 in Todorovska and Trifunac 2007) and indirect analyses of the nonlinear waves in the VN7SH (Gicev and Trifunac 2006b; Todorovska and Trifunac 2006d), and show trends similar to what has been seen in other buildings damaged by strong motion waves (Todorovska and Trifunac 2006a,b,c).

4. SUMMARY AND CONCLUSIONS

Biot's response spectrum method uses characteristic functions (mode shapes) to represent vibration of multi-degree-of-freedom system via a set of equivalent single-degree-of-freedom oscillators. Superposition of modal responses is then used to compute actual system response, and the peak of that response is employed in earthquake resistant design, to construct envelopes of maximum relative responses (thus defining maximum drift), or of maximum inter-story forces. Mathematically this approach is complete, and the representation in terms of modal responses converges to the exact linear response. However, the simplifications imposed by the design practice, result in the use of only the lowest modes of response. The consequence is that the amplitudes of dynamic response to sudden, high frequency excitation by a near-field pulse are seriously underestimated. For large strong motion amplitudes the above approach breaks down as the representation in terms of a superposition of modal responses ceases to be valid for non-linear response.

When the motion of the structure can be approximated by one-dimensional shear beam (i.e. the contribution of rotational waves can be neglected), we have shown how by comparing the power of a pulse entering the structure (demand) with the ability of structure to absorb this power (capacity), can lead to simple and direct estimation of the required structural capacity.

Power (energy and its duration) of the strong near-field pulses will determine whether the wave entering the structure will continue to propagate through the structure as a linear wave, or will begin to create non-linear zones (at first near top, and/or near base of the structure; Gicev, 2005). For high frequency pulses the non-linear zone, with permanent strains, can be created before the wave motion reaches the top of the structure, that is before the interference of waves has even started to occur leading to formation of mode shapes. Overall duration of strong motion (Trifunac and Novikova, 1994) will determine the number of times the structure may be able to complete full cycles of response, and the associated number of "minor" excursions into the non-linear response range, when the response is weakly non-linear (Gupta and Trifunac, 1996), while the presence of powerful pulses of strong motion will determine the extent to which the one-directional quarter period responses may lead to excessive ductility demand, leading to dynamic instability and failure, precipitated by the gravity loads (Husid, 1967). All these possibilities can be examined and quantified deterministically by computation of the associated power capacities and power demands, for different scenarios, for given recorded or synthesized strong motion accelerograms, or probabilistically by extending the methods developed for Uniform Hazard Analysis [Todorovska et al., 1995].

5. REFERENCES

1. Akiyama, H. (1985). Earthquake-Resistant Limit-State Design for Buildings, *Univ. of Tokyo Press*, Tokyo, Japan.
2. Arias, A. (1970). A Measure of Earthquake Intensity, in "Seismic Design of Nuclear Power Plants", R.J. Hansen (editor), The Mass. Inst. of Tech. Press.
3. Benioff, H. (1934). The Physical Evaluation of Seismic Destructiveness, *Bull. Seism. Soc. Amer*., **24**, 398-403.

4. Biot, M.A. (1932). Vibrations of Building During Earthquake, Chapter II in *Ph.D. Thesis No.* 259 entitled "Transient Oscillations in Elastic Systems", Aeronautics Department, Calif. Inst. of Tech., Pasadena, California.

5. Biot, M.A. (1933). Theory of Elastic Systems Vibrating Under Transient Impulse with an Application to Earthquake – Proof Buildings, *Proc. National Academy of Sciences*, **19**(2), 262-268.

6. Biot, M.A. (1934). Theory of Vibration of Buildings During Earthquake, *Zeitschrift für Angewandte Matematik und Mechanik*, **14**(4), 213-223.

7. Biot, M.A. (1941). A Mechanical Analyzer for the Prediction of Earthquake Stresses, *Bull. Seism. Soc. Amer*., **31**(2), 151-171.

8. Biot, M.A. (1942). Analytical and Experimental Methods in Engineering Seismology, *ASCE, Transactions*, **108**, 365-408.

9. Blume, J.A., and Assoc. (1973). Holiday Inn, Chapter 29 *in San Fernando, California Earthquake of February 9, 1971,* Vol. I, Part A, U.S. Dept. of Commerce, National Oceanic and Atmospheric Administration, Washington, D.C.

10. Browning, J.A., Li, R.Y., Lynn, A., and Moehle, J.P. (2000). Performance assessment for a reinforced concrete frame building, *Earthquake Spectra*, *16*(3), 541–555.

11. De la Llera, J.C., Chopra, A.K., and Almazan, J.L. (2001). Three-dimensional inelastic response of an RC building during the Northridge earthquake. *J. of Structural Eng., ASCE*, 127(5), 482–489.

12. Fajfar, P. and Krawinkler, H. (editors) (1992). Nonlinear Seismic Analysis and Design of Reinforced Concrete Buildings, *Elsevier Applied Science*, London, New York.

13. Gicev, V. (2005). Investigation of soil-flexible foundation-structure interaction for incident plane SH waves, *Ph.D. Dissertation*, Dept. of Civil Engineering, Univ. Southern California, Los Angeles, California.

14. Gicev, V. and Trifunac, M.D. (2006a)*. Rotations in the Transient Response of Nonlinear Shear Beam, *Dept. of Civil Eng. Report CE 06-02,* Univ. of Southern California, Los Angeles, California.

15. Gicev, V. and Trifunac, M.D. (2006b)*. Non-Linear Earthquake Waves in Seven-Story Reinforced Concrete Building, *Dept. of Civil Eng. Report CE 06-03,* Univ. of Southern California, Los Angeles, California.

16. Gupta, I.D. and Trifunac, M.D. (1996)*. Investigation of Nonstationarity in Stochastic Seismic Response of Structures, *Dept. of Civil Eng. Report CE 96-01*, Univ. of Southern California, Los Angeles, California

17. Gutenberg, B. and Richter, C.F. (1956a) Earthquake Magnitude, Intensity, Energy, and Acceleration, *Bull. Seism. Soc. Amer*., **46**(2), 105-145.

18. Gutenberg, B. and Richter, C.F. (1956b). Magnitude and Energy of Earthquakes, *Ann. Geofisica*, **9**, 1-15.

19. Hayir, A., Todorovska, M.I. and Trifunac, M.D. (2001). Antiplane Response of a Dike with Flexible Soil-Structure Interface to Incident SH-waves, *Soil Dynam. and Earthquake Eng*., **21**(7), 603-613.

20. Husid, R. (1967). Gravity Effects on the Earthquake Response of Yielding Structures, *Ph.D. Thesis*, Calif. Inst. of Tech., Pasadena, California.

21. Islam, M.S. (1996). Analysis of the Response of an Instrumented 7-story Nonductile Concrete Frame Building Damaged During the Northridge Earthquake, *Professional Paper 96-9*, Los Angeles Tall Buildings Structural Design Council.

22. Ivanović, S.S., Trifunac, M.D., Novikava, E.I., Gladkov, A.A., & Todorovska, M.I. (1999a)*. Instrumented 7-story Reinforced Concrete Building in Van Nuys, California: Ambient Vibration Surveys Following the Damage from the 1994 Northridge Earthquake. Dept. of Civil Eng., *Rep. No. CE 99-03*, Univ. of Southern California, Los Angeles, California.

23. Ivanović, S., Trifunac, M.D., and Todorovska, M.I. (1999b). On identification of damage in structures via wave travel times. *Proc. NATO Workshop on Strong Motion Instrumentation for Civil Engineering Structures,* June 2–5, Istanbul, Turkey, Kluwer Academic Pub., Dordrecht , (2001), 447–468.

24. Ivanović, S.S., Trifunac, M.D., Novikava, E.I., Gladkov, A.A., & Todorovska, M.I. (2000). Ambient Vibration Tests of a Seven-Story Reinforced Concrete Building in Van Nuys, California, Damaged by the 1994 Northridge Earthquake. *Soil Dynam. and Earthquake Engrg*., **19**(6), 391-411.

25. Joyner, W.B. (1975). A Method for Calculating Nonlinear Seismic Response in Two Dimensions, *Bull. Seism. Soc. Amer*., **65**(5), 1337-1357.

26. Joyner, W.B. and Chen, A.T.F. (1975). Calculating of Nonlinear Ground Response in Earthquakes, *Bull. Seism. Soc. Amer*., **65**(5), 1315-1336.

27. Kanai, K. (1965). Some problems of seismic vibration of structures, Proc. Third World Conf. Earthquake Eng., New Zealand, Vol. II, 260-275.

28. Lee, V.W. (1979)*. Investigation of Three-Dimensional Soil-Structure Interaction, *Report No. CE 79-11*, Dept. of Civil Eng., University of Southern California, Los Angeles, California.

29. Li, R.Y. and Jirsa, J.D. (1998). Nonlinear Analysis of an Instrumented Structure Damaged in the 1994 Northridge Earthquake, *Earthquake Spectra*, **14**(2), 265-283.

30. Luco, J.E., M.D. Trifunac and Wong, H.L. (1985)*. Soil Structure Interaction Effects on Forced Vibration tests, Dept. of Civil Eng. *Report No. 86-05*, Univ. of Southern California, Los Angeles, California.

31. Mulhern, M.R., and Maley, R.P. (1973). Building Period Measurements Before, During And After the San Fernando, California, Earthquake of February 9, 1971, *U.S. Depart. Of Commerce, National Oceanic and Atmospheric Administration,* Washington D.C., Vol. I, Part B, 725–733.

32. Safak, E. (1998). New Approach to Analyzing Soil-Building Systems, *Soil Dynam. and Earthquake Eng*,, **17**, 509-517.

33. Todorovska, M.I., and Lee, V.W. (1989). Seismic Waves in Buildings with Shear Walls or Central Core, *J. Engrg. Mech*., ASCE, **115**(12), 2669-2686.

34. Todorovska, M.I., and Trifunac, M.D. (1989). Antiplane Earthquake Waves in Long Structures, *J. of Engrg. Mech*., ASCE, **115**(12), 2687-2708.

35. Todorovska, M.I., and Trifunac, M.D. (1990a). A Note on the Propagation of Earthquake Waves in Buildings with Soft First Floor, *J. of Engrg. Mech*., ASCE, **116**(4), 892-900.

36. Todorovska, M.I., and Trifunac, M.D. (1990b). A Note on Excitation of Long Structures by Ground Waves, *J. of Engrg Mech*., ASCE, **116**(4), 952-964.

37. Todorovska, M.I. and Trifunac, M.D. (1991)*. Radiation Damping During Two-Dimensional Building-Soil Interaction, Dept. of Civil Eng., *Rep. No. 91-01*, Univ. of Southern California, Los Angeles, California.

38. Todorovska, M.I. and Trifunac, M.D. (1992). The System Damping, the System Frequency and the System Response peak Amplitudes during in-plane Building-Soil Interaction, *Earthquake Eng. and Struct. Dynam.*, **21**(2), 127-144.

39. Todorovska, M.I. and Trifunac, M.D. (1993)*. The Effects of Wave Passage on the Response of Base-Isolated Buildings on Rigid Embedded Foundations, Dept of Civil Eng., *Report No. CE 93-10*, Univ. of Southern California, Los Angeles, California.

40. Todorovska, M.I., and Trifunac, M.D. (2006a). Damage detection in the Imperial County Services Building I: The data and time-frequency analysis, *Soil Dynamics and Earthquake Eng*., (in press).

41. Todorovska, M.I., and Trifunac, M.D. (2006b). Damage detection in the Imperial County Services Building II: Analysis of novelties via wavelets (submitted for publication).

42. Todorovska, M.I., and Trifunac, M.D. (2006c). Earthquake damage detection in the imperial county services building III: Analysis of wave travel times via impulse response functions (submitted for publication).

43. Todorovska, M.I., and Trifunac, M.D. (2006d). Impulse response analysis of the Van Nuys 7-story hotel during 11 earthquakes (1971-1994): one-dimensional wave propagation and inferences on global and local reduction of stiffness due to earthquake damage, Report CE 06-01, Dept. of Civil Eng., University of Southern California, Los Angeles, California.

44. Todorovska, M.I. and Trifunac, M.D. (2007). Impulse Response Analysis of the Van Nuys 7-Story Hotel During 11 Earthquakes and Earthquake Damage Detection, *Structural Control and Health Monitoring* (in press).

45. Todorovska, M.I., Trifunac, M.D. , and Lee, V.W. (1988)*. Investigation of Earthquake Response of Long Buildings, Dept of Civil Engrg, *Report No. CE 88-02*, Univ. of Southern California, Los Angeles, California.

46. Todorovska, M.I., Gupta, I.D., Gupta, V.K., Lee, V.W., and Trifunac, M.D. (1995)*. Selected Topics in Probabilistic Seismic Hazard Analysis, *Dept. of Civil Eng. Report CE 95-08*, Univ. of Southern California, Los Angeles, California.

47. Todorovska, M.I. Ivanovic, S.S. and Trifunac, M.D. (2001a). Wave Propagation in a Seven-Story Reinforced Concrete Building, Part I: Theoretical Models, *Soil Dynam. and Earthquake Eng*., **21**(3), 211-223.

48. Todorovska, M.I. Ivanovic, S.S. and Trifunac, M.D. (2001b). Wave Propagation in a Seven-Story Reinforced Concrete Building, Part II: Observed Wave Numbers, *Soil Dynam. and Earthquake Eng*., **21**(3), 211-223.

49. Todorovska, M.I., Hayir, A. and Trifunac, M.D. (2001c). Antiplane Response of a Dike on Flexible Embedded Foundation to Incident SH-Waves, *Soil Dynam. and Earthquake Eng*., **21**(7), 593-601.

50. Trifunac, M.D. (1994). Q and High Frequency Strong Motion Spectra, *Soil Dynam. and Earthquake Eng*., **13**(3), 149-161.

51. Trifunac, M.D. (2003)*. 70-th Anniversary of Biot Spectrum, 23-rd Annual ISET Lecture, *Indian Society of Earthquake Technology*, Vol. 40, No. 1, 19-50.

52. Trifunac, M.D. (2005). Scientific citations of M. A. Biot, Proc. Biot centennial conference, Norman, Oklahoma, in *Poromechanics III,* Edited by Abousleiman, Y.N., Cheng, A.H., and Ulm, F.J., 11-17, (2005).

53. Trifunac, M.D. and Brady, A.G. (1975). A Study of the Duration of Strong Earthquake Ground Motion, *Bull. Seism. Soc. Amer*., **65**, 581-626.

54. Trifunac, M.D., and Hao, T.Y. (2001)*. 7-Story Reinforced Concrete Building in Van Nuys, California: Photographs of the Damage from the 1994 Northridge Earthquake, *Dept. of Civil Eng. Report No. CE 01-05.* Univ. of Southern California, Los Angeles, California.

55. Trifunac, M.D., and Ivanovic, S.S. (2003)*. Analysis of Drifts in a Seven-Story Reinforced Concrete Structure, *Dept. of Civil Eng. Report No. CE 03-01*, Univ. of Southern California, Los Angeles, California.

56. Trifunac, M.D. and Novikova, E.I., (1994). State of the Art Review on Strong Motion Duration, *10th European Conf. on Earthquake Eng*., Vol. I, 131-140.

57. Trifunac, M.D. and Todorovska, M.I. (1996). Nonlinear Soil Response – 1994 Northridge California, Earthquake, *J. Geotechnical Eng.,* ASCE, **122**(9), 725-735.

58. Trifunac, M.D. and Todorovska, M.I. (1998a). Nonlinear Soil Response as a Natural Passive Isolation Mechanism – The 1994 Northridge, California Earthquake, *Soil Dynam. and Earthquake Eng*., **17**(1), 41-51.

59. Trifunac, M.D., and Todorovska, M.I. (1998b). "Damage distribution during the 1994 Northridge, California, earthquake in relation to generalized categories of surface geology", *Soil Dynam. and Earthquake Engrg,* 17(4), 238-252.

60. Trifunac, M.D. and Todorovska, M.I. (1999). Reduction of Structural Damage by Nonlinear soil Response, *J. Structural Eng.,* ASCE, 125(1), 89-97.

61. Trifunac, M.D. and Todorovska, M.I. (2001). Recording and Interpreting Earthquake Response of Full-Scale Structures, Proc. NATO Workshop on Strong Motion Instrumentation for Civil Engineering Structures, June 2-5, 1999, Instanbul, Turkey, M. Erdik et al. (eds.), *Kluwer Academic Publishers*, 131-155.

62. Trifunac, M.D., Ivanovic, S.S., Todorovska, M.I., Novikova, E.I. and Gladkov, A.A. (1999a). Experimental Evidence for Flexibility of a Building Foundation Supported by Concrete Friction Piles, *Soil Dynam. and Earthquake Eng*., **18**(3), 169-187.

63. Trifunac, M.D., Ivanovic, S.S. and Todorovska, M.I. (1999b)*. Seven Story Reinforced Concrete Building in Van Nuys, California: Strong Motion Data Recorded Between 7 February 1971 and 9 December 1994, and Description of Damage Following Northridge, 17 January 1994 Earthquake, Dept. of Civil Eng., *Rep. No. 99-02*, Univ. of Southern California, Los Angeles, California.

64. Trifunac, M.D., Ivanovic, S.S. and Todorovska, M.I. (2001a). Apparent Periods of a Building, Part I: Fourier Analysis, *J. of Structural Eng*., ASCE, **127**(5), 517-526.

65. Trifunac, M.D., Ivanovic, S.S. and Todorovska, M.I. (2001b). Apparent Periods of a Building, Part II: Time-Frequency Analysis, *J. of Structural Eng*., ASCE, **127**(5), 527-537.

66. Trifunac, M.D., Ivanovic, S.S. and Todorovska, M.I. (2001c). Wave Propagation in a Seven-story Reinforced Concrete Building, III: Damage Detection Via Changes in Wave Numbers, *Soil Dynam. and Earthquake Eng.*, **23**(1), 65-75.

67. Trifunac, M.D., Hao, T.Y. and Todorovska, M.I. (2001d)*. On Energy Flow in Earthquake Response, Dept. of Civil Eng., *Report No. CE 01-03*, Univ. of Southern California, Los Angeles, California.

68. Uang, C.M., & Bertero, V.V. (1988). Use of Energy as a Design Criterion in Earthquake-Resistant Design. *Report No. UCB/EERC-88/18*, Earthquake Engineering Research Center, University of California, Berkeley, California.

69. Veletsos, A.S., and Newmark, N.M. (1960). Effects of Inelastic Behavior on the Response of Simple Systems to Earthquake Motions, *Proceed. 2nd World Conf. on Earthquake Engrg,* Tokyo, Japan, Vol. II, 895-912.

---

*Can be downloaded from: http://www.usc.edu/dept/civil_eng/Earthquake_eng/